Macromolecules **1999,** *32,* 8465−8475

Annealing Effect of Microphase-Separated Membranes Containing Poly(dimethylsiloxane) on Their Permselectivity for Aqueous Ethanol Solutions

Takashi Miyata,* Seiji Obata, and Tadashi Uragami*

Chemical Branch, Faculty of Engineering and High Technology Research Center, Kansai University, Suita, Osaka 564-8680, Japan

Received June 16, 1999

ABSTRACT: The annealing effects of block and graft copolymer membranes consisting of ethanol-permselective poly(dimethylsiloxane) (PDMS) plus water-permselective poly(methyl methacrylate) (PMMA) on their permselectivity for an aqueous ethanol solution in pervaporation were investigated in terms of their microphase separation. The ethanol-permselectivity of the block copolymer membranes was strongly influenced by the annealing, but that of the graft copolymer membranes was not. The original block copolymer membranes changed from water- to ethanol-permselectivity at a DMS content of 55 mol %, but the annealed block copolymer membranes changed at a DMS content of 37 mol %. Transmission electron micrography demonstrated that the annealing of the block copolymer membranes with a DMS content between 37 and 55 mol % resulted in dramatic changes in the morphology of their microphase separation. However, the annealing of the graft copolymer membranes had very little effect on the morphology of their microphase separation, which was quite different from the morphology of the block copolymer membranes. The analysis using a combined model consisting of parallel and series models revealed that a continuous PDMS phase in the direction of the membrane thickness is readily formed by the annealing of the block copolymer membranes. As a result, the continuity of the PDMS phase in the microphase separation governed the ethanol-permselectivity of these membranes for an aqueous ethanol solution. This report concludes that the morphological design of microphase-separated membranes, which can be achieved by membrane annealing, is very important in controlling their permeability and permselectivity.

Introduction

Membrane techniques have many advantages in terms of potential savings in energy costs for the separation of organic liquid mixtures such as alcohol/water, benzene/cyclohexane, etc., which have some difficulties in separation by distillation despite their high potential as valuable fuels and raw materials. Pervaporation is a highly promising technique for the separation of such organic liquid mixtures.[1] Many researchers have prepared pervaporation membranes from hydrophilic or hydrophobic polymers to separate aqueous ethanol solutions, hydrocarbon mixtures, and so on.[2−7] We have investigated the pervaporation characteristics of chemically modified chitosan membranes,[8−11] poly(dimethylsiloxane) (PDMS) derivative membranes,[12−19] cyclodextrin-containing polymer membranes,[20,21] and liquid crystalline polymer membranes[22−25] for the separation of various organic liquid mixtures. The previous studies revealed that chemical and physical structures of their membranes strongly influence their permeability and permselectivity for organic liquid mixtures in pervaporation. In addition, it was apparent that polymer membranes containing a variety of components have high potential as pervaporation membranes because the membrane structures can be easily controlled by the kind of component or composition.

Multicomponent polymers have attracted considerable attention in the industrial field, because these compounds combine a variety of functional components into a single material.[26−30] In membrane techniques, also, multicomponent polymers are promising membrane materials because the membrane performance can be controlled by a variety of functional components. Most multicomponent polymer membranes show micro- or macrophase separation due to the very small entropy and positive heat of mixing. The morphology of such phase separation in multicomponent polymer membranes must influence their permeability and permselectivity because the solubility and diffusivity of permeants in the membranes are closely associated with the morphology. Therefore, relating microphase separation in multicomponent polymer membranes to their permeability and permselectivity is of great importance for the development of polymer membranes with high performance. There were a few reports on gas permeation through microphase-separated membranes, which focused on the relationship between their morphology and gas permeability.[31−43] However, very few reports on pervaporation membranes have described the effects of microphase separation on the permselectivity in pervaporation membranes for the separation of organic liquid mixtures. Kerres et al.[44] reported that morphological changes in multicomponent polymer membranes caused a drastic change in their permselectivity at the percolation point. Their study revealed the importance of examining the relationship between microphase separation in pervaporation membranes and their permselectivity for organic liquid mixtures, because microphase separation has a more marked influence on permeability and permselectivity in pervaporation membranes than in gas permeation membranes. Furthermore, fundamental research on the microphase separation and permselectivity of multicomponent polymer

---

* To whom correspondence should be addressed.

10.1021/ma9909612 CCC: $18.00

Chart 1

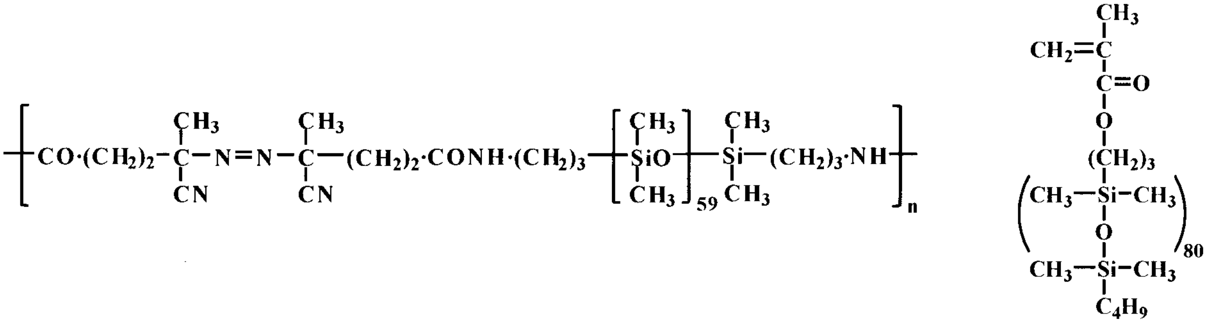

$$\left[-CO\cdot(CH_2)_2-\underset{CN}{\overset{CH_3}{C}}-N=N-\underset{CN}{\overset{CH_3}{C}}-(CH_2)_2\cdot CONH\cdot(CH_2)_3-\left[\underset{CH_3}{\overset{CH_3}{Si}}O\right]_{59}-\underset{CH_3}{\overset{CH_3}{Si}}-(CH_2)_3\cdot NH- \right]_n$$

PDMS macro-azo-initiator (1)

PDMS macromonomer (2)

membranes will lead to a better understanding of the pervaporation process during the separation of organic liquid mixtures.

We have studied the relationship between structure and properties of multicomponent polymer membranes in order to develop high-performance pervaporation membranes for the separation of aqueous ethanol solutions.[12−19] The main point of our studies has been to relate the morphology of microphase-separated membranes to their permeability and permselectivity for organic liquid mixtures. It was apparent from our previous studies that the permselectivity of microphase-separated membranes consisting of ethanol- and water-permselective components is strongly governed by the continuity of each phase.[12−14] Furthermore, the difference in morphology of microphase separation between block and graft copolymer membranes resulted in their quite different pervaporation characteristics despite their same composition.[19] These suggest that designing the morphology of microphase-separated membranes is of great importance for controlling their permeability and permselectivity in pervaporation. These investigations into multicomponent pervaporation membranes have also contributed significantly to our understanding of the permeation mechanisms in pervaporation, which is fundamental for developing high-performance pervaporation membranes.

The purpose of our studies is to reveal the universal relationship between the morphology of the microphase separation in two-component polymer membranes consisting of ethanol- and water-permselective components and their permeability and permselectivity for aqueous ethanol solutions during pervaporation. This paper focuses on the annealing effect on the morphology of microphase separation in two-component polymer membranes consisting of ethanol- and water-permselective components. Furthermore, the permeability and permselectivity of the annealed membranes are discussed on the basis of morphological changes in microphase separation following the annealing. In this study, block and graft copolymer membranes consisting of ethanol-permselective PDMS and water-permselective poly(methyl methacrylate) (PMMA) were prepared by the polymerization of methyl methacrylate (MMA) with a PDMS macro-azo-initiator and by the copolymerization of MMA with a PDMS macromonomer, respectively, according to methods previously reported.[12,14,18,19] The annealing effects on the pervaporation characteristics of two types of copolymer membranes were investigated in more detail from the perspective of their different morphology resulting from different molecular architecture.

Experimental Section

Materials. The poly(dimethylsiloxane) (PDMS) macro-azo-initiator (PASA)[45−47] **(1)**, which has 59 units of the PDMS block subunit, was supplied by Wako Pure Chemical Industries, Ltd. The PDMS macromonomer, which has 81 units of the pendant PDMS (**2**), was supplied by Toray Dow Corning Silicone Co., Ltd. (see Chart 1). Methyl methacrylate (MMA) monomer was purified by distillation under reduced pressure in nitrogen gas. All other solvents and reagents were of analytical grade and were obtained from commercial sources and used without further purification.

Synthesis of Two Types of Copolymers and Their Membrane Preparation. Block copolymers consisting of PDMS and PMMA (PMMA-*b*-PDMS) were synthesized by the polymerization of MMA with a PDMS macro-azo-initiator according to previous reports.[19] Graft copolymers consisting of PDMS and PMMA (PMMA-*g*-PDMS) were obtained by the copolymerization of a PDMS macromonomer with MMA by the methods reported in previous papers.[12,14] The composition and average molecular weights of the resultant PMMA-*b*-PDMS and PMMA-*g*-PDMS have been summarized in previous papers.[14,19]

The prescribed amounts of PMMA-*b*-PDMS and PMMA-*g*-PDMS were dissolved in benzene at 25 °C to a concentration of 4 wt % for the preparation of the casting solutions. The PMMA-*b*-PDMS and PMMA-*g*-PDMS membranes were prepared by pouring the casting solutions onto rimmed glass plates and then allowing the solvent to evaporate completely at 25 °C. The resultant membranes were transparent, and their thickness was about 40 μm. Furthermore, annealed membranes were obtained by keeping the PMMA-*b*-PDMS and PMMA-*g*-PDMS membranes in an oven at various temperatures for 2 h.

Transmission Electron Micrographs (TEM). The PMMA-*b*-PDMS and PMMA-*g*-PDMS membranes before and after the annealing were vapor-stained with an aqueous solution of 5 wt % RuO_4 in glass-covered dishes.[48] The stained membranes were then embedded in epoxy resin and cross sectioned into thin films (thickness: approximately 60 nm) with a microtome (Leica; Reichert Ultracut E). The morphological features that were highlighted by our staining procedure were observed with a transmission electron microscope (TEM) (JEOL JEM-1210) at an accelerating voltage of 80 kV.

Permeation Measurements. Pervaporation was performed using the apparatus described in previous papers[12−19] under the following conditions: permeation temperature, 40 °C; pressure on the permeate side, 1×10^{-2} Torr. The effective membrane area was 13.8 cm^2. An aqueous solution of 10 wt % ethanol was used as the feed solution. The compositions of the feed solution and permeate were determined by a gas chromatograph (Shimadzu GC-9A) equipped with a flame ionization detector (FID) and a capillary column (Shimadzu Co. Ltd.; Shimalite F) heated to 200 °C. The permeation rates of an aqueous ethanol solution during pervaporation were determined from the weight of the permeate collected in a cold trap,

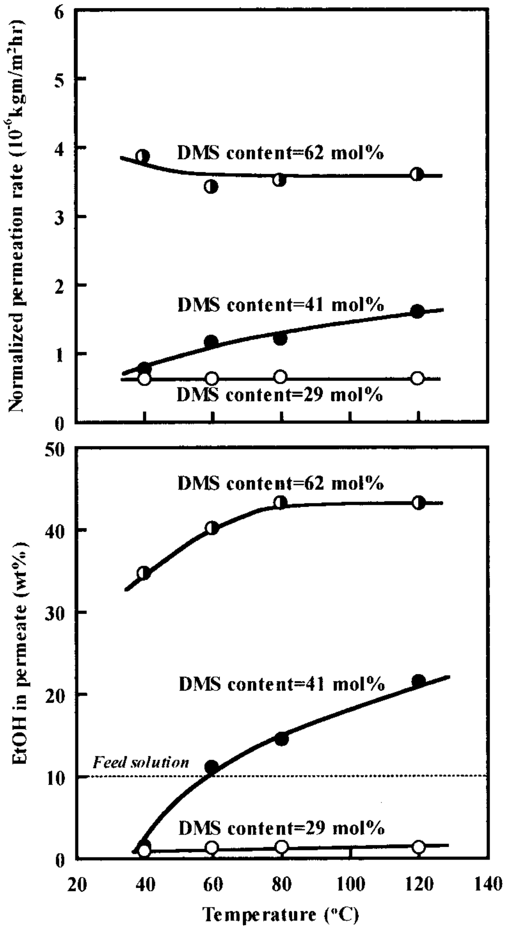

Figure 1. Effects of the annealing temperature on the ethanol concentration of the permeate and on the normalized permeation rate through the annealed PMMA-*b*-PDMS membranes with DMS contents of 29 (○), 41 (●), and 62 mol % (◑) during pervaporation. The feed solution was an aqueous solution of 10 wt % ethanol (40 °C). The dashed line represents the feed composition.

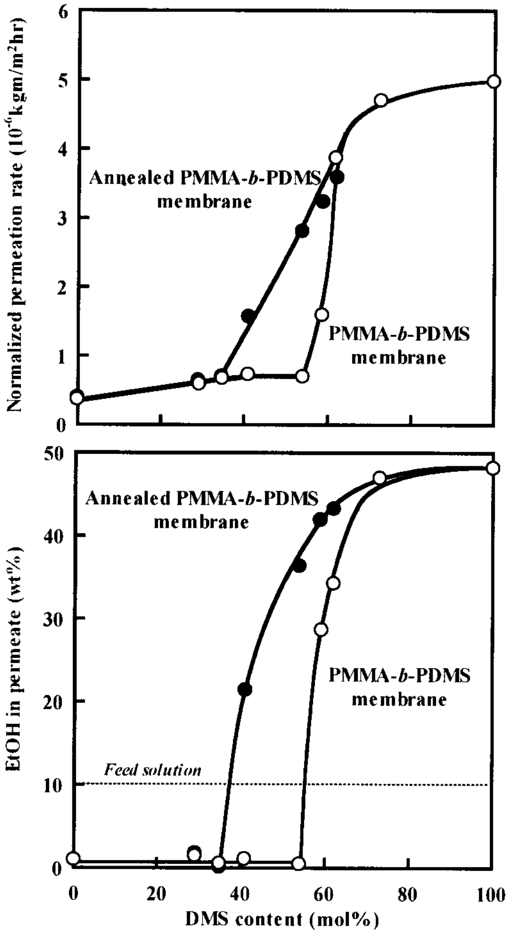

Figure 2. Effects of the DMS content on the ethanol concentration of the permeate and on the normalized permeation rate through the PMMA-*b*-PDMS membranes (○) and their annealed membranes (120 °C, 2 h) (●) during pervaporation. The feed solution was an aqueous solution of 10 wt % ethanol (40 °C). The dashed line represents the feed composition.

the permeation time, and the effective membrane area. The results of the permeation of an aqueous ethanol solution by pervaporation were reproducible, and the errors inherent in the permeation measurements were of the order of a few percent.

Results and Discussion

Effect of Annealing on Pervaporation Characteristics of PMMA-*b*-PDMS Membranes. Figure 1 shows the annealing temperature dependence of the ethanol concentration in the permeate and the normalized permeation rate of an aqueous solution of 10 wt % ethanol through the annealed PMMA-*b*-PDMS membranes. In this figure, the normalized permeation rate that is the product of the permeation rate and the membrane thickness is used for evaluating the essential permeability of the membrane. The normalization of the permeation rate can reveal the detailed relationship between the membrane structure and the permeability. In this study, there is no appreciable change in the membrane thickness through the annealing process. With rising annealing temperature, the normalized permeation rate through the PMMA-*b*-PDMS membranes with a DMS content of 29 and 62 mol % was constant, but that through the membrane with a DMS content of 41 mol % increased. On the other hand, the ethanol concentration of the permeate passing through PMMA-*b*-PDMS membrane with a DMS content of 29 mol % was generally less than 10 wt %. This result suggests that all the annealed block copolymer membranes with a DMS content of 29 mol % are water-permselective, regardless of the annealing temperature. In the membranes with a DMS content of 41 and 62 mol %, however, increasing the annealing temperature led to an increase in the ethanol concentration in the permeate. It is worth noting that the annealed membrane with a DMS content of 41 mol % changed from water- to ethanol-permselectivity due to rising annealing temperature. This implies that the permselectivity of the PMMA-*b*-PDMS membrane can be controlled by the annealing.

Figure 2 shows the effects of the DMS content of the original PMMA-*b*-PDMS membranes and the PMMA-*b*-PDMS membranes annealed at 120 °C for 2 h on the ethanol concentration in the permeate and on the normalized permeation rate of an aqueous solution of 10 wt % ethanol through the membranes. In the PMMA-*b*-PDMS membranes with a DMS content of less than 37 mol %, no appreciable effect of the annealing on the ethanol concentration in the permeate and normalized permeation rate was observed. Some researchers reported that permeation characteristics of glassy polymer membranes are strongly influenced by the annealing because the glassy polymers are nonequilibrium materials.[49,50] In this study, however, the permeation characteristics of the PMMA-*b*-PDMS membranes with a DMS content of less than 37 mol % did not change by the annealing as our annealing time of 2 h was much shorter than the annealing time reported previously by the researchers. The original and annealed PMMA-*b*-PDMS membranes showed an abrupt increase in the normalized permeation rate at a DMS content of 55 and 37 mol %, respectively. Because the PDMS component is rubbery and the PMMA component is glassy, the diffusivity of the permeants in the former is much higher than in the latter.[51−53] The much higher diffusivity in the PDMS component causes an increase in the normalized permeation rate with increasing DMS content. Similarly, the ethanol concentration of the permeate through the original and annealed PMMA-*b*-PDMS membranes increased dramatically with an increase in the DMS content of more than 55 and 37 mol %, respectively. An increase in the ethanol concentration of the permeate is based on the fact that the ethanol-permselectivity of the PDMS component becomes more predominant than the water-permselectivity of the PMMA component. In addition, the original PMMA-*b*-PDMS membranes with a DMS content of less than 55 mol % are water-permselective and the original membranes of more than 55 mol % are ethanol-permselective, but the annealed PMMA-*b*-PDMS membranes changed from water- to ethanol-permselective at a DMS content of about 37 mol %. Namely, the threshold DMS content at which the annealed PMMA-*b*-PDMS membranes change from water- to ethanol-permselective is quite different from the threshold DMS content of the original membranes. It is quite obvious that the original PMMA-*b*-PDMS membranes are water-permselective whereas the annealed PMMA-*b*-PDMS membranes are ethanol-permselective at a DMS content between 37 and 55 mol %. These results suggest that the permeability and permselectivity of multicomponent polymer membranes containing PDMS can be controlled by the annealing without changing the polymer composition. To determine the reason why the annealing shifted the threshold DMS content at which the membrane characteristics changed dramatically, we focused on the differences in membrane structures in the next section.

(a) Air-side surface

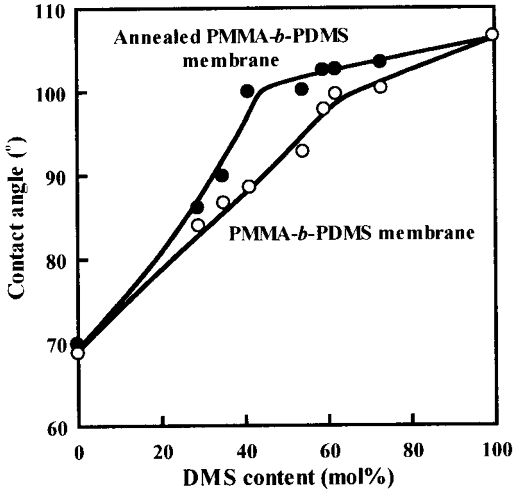

(b) Glass-side surface

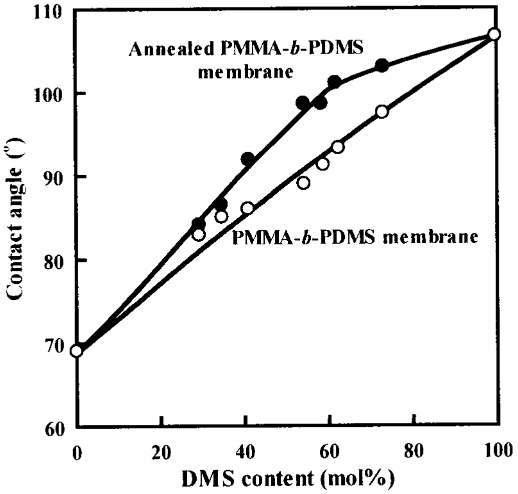

Figure 3. Effects of the DMS content on the contact angle of water on the air-side surface (a) and glass-side surface (b) of PMMA-*b*-PDMS membranes (○) and their annealed membranes (120 °C, 2 h) (●).

Structural Changes in PMMA-*b*-PDMS Membranes Due to Annealing. Figure 3 shows the relationship between the DMS content and the contact angles of water on air-side and glass-side surfaces of the original PMMA-*b*-PDMS membranes and the PMMA-*b*-PDMS membranes annealed at 120 °C for 2 h. The contact angles of water on both the surfaces of the original and annealed PMMA-*b*-PDMS membrane increased gradually with increasing DMS content. This is attributed to the fact that the PDMS component is more hydrophobic than the PMMA component. In both membranes, the air-side surface showed a sharper increase in the contact angle than the glass-side surface by the introduction of a PDMS component. This indicates that their air-side surfaces are more hydrophobic than their glass-side surfaces. It is concluded from these results that the PDMS component is preferentially concentrated at the air-side surfaces of both the original and annealed PMMA-*b*-PDMS membranes to minimize their surface free energy for a thermodynamically stable state during the membrane formation. The difference in the surface characteristics between the air-side surface and the glass-side surface led us to the anticipation that their membranes are heterogeneous in the distribution of each component. In addition, the annealing of the PMMA-*b*-PDMS membranes made both the air-side and glass-side surfaces more hydrophobic. This demonstrates that more PDMS component migrated to the membrane surfaces to minimize their surface free energy by the annealing. From the effect of the annealing on the contact angles, it is concluded that the annealing at 120 °C enhances the mobility of polymer chains and enables them to reorganize. These results have led us to speculate that the annealing can lead to reconstruction of the membrane structures that influence membrane characteristics strongly.

Transmission electron micrographs of cross sections of the PMMA-*b*-PDMS membranes with various DMS contents are shown in Figure 4. The PDMS component was stained by RuO_4, but the PMMA component was not. These micrographs clearly demonstrate that all of the original and annealed PMMA-*b*-PDMS membranes had distinct microphase separation consisting of a PDMS phase and a PMMA phase. The morphology of the microphase separation was strongly dependent upon the DMS content. The morphology of the original PMMA-*b*-PDMS membranes with a DMS content of more than 62 mol % was quite different from those of

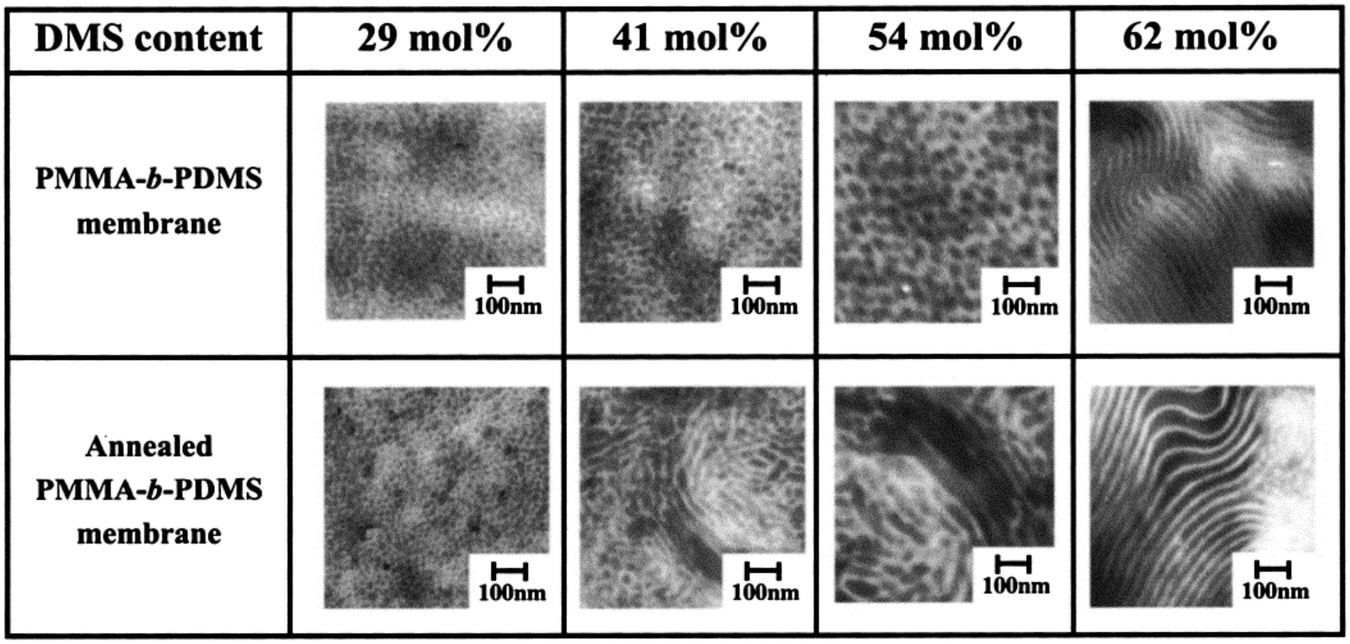

Figure 4. Transmission electron micrographs of cross sections of the PMMA-*b*-PDMS membranes and their annealed membranes (120 °C, 2 h) with various DMS contents. The dark region stained by RuO_4 represents the PDMS component.

less than 54 mol %. On the other hand, the morphology of the annealed PMMA-*b*-PDMS membranes changed dramatically at a DMS content of about 41 mol %, differing from that of the original membranes. It is worth noting that the annealing led to a dramatic change in morphology of the PMMA-*b*-PDMS membranes with a DMS content between 41 and 54 mol %. The original PMMA-*b*-PDMS membranes with a DMS content of less than 54 mol % had a microphase separation consisting of a discontinuous PDMS phase and a continuous PMMA phase, but the original membranes of more than 62 mol % had bicontinuous PDMS and PMMA phases. On the other hand, the annealing of the PMMA-*b*-PDMS membranes with a DMS content of 41 and 54 mol % enlarged the PDMS phase until it formed a continuous phase. The threshold DMS content at which the permeability and permselectivity changed remarkably in both the original and annealed PMMA-*b*-PDMS membranes corresponded to the DMS content at which the morphology in their microphase separation changed dramatically from a discontinuous PDMS phase to a continuous PDMS phase. This suggests that the morphological change in the microphase separation of the PMMA-*b*-PDMS membranes by annealing causes the drastic changes in their permeability and permselectivity for an aqueous ethanol solution. Therefore, the results of pervaporation for an aqueous ethanol solution must be evaluated in more detail from the perspective of morphological changes in the PMMA-*b*-PDMS membranes.

Structural Models for Permeability of Annealed PMMA-*b*-PDMS Membranes. Previous studies have revealed that discussion using a combined model consisting of a series model plus a parallel model is very useful in quantitatively analyzing the morphological changes of membrane microphase separation.[14,19] Therefore, the permeation rates of an aqueous ethanol solution through the original and annealed PMMA-*b*-PDMS membranes were discussed for a more detailed investigation of membrane morphology according to the method previously reported.[14,19] In the combined model, the PMMA phase is divided into a PMMA1 phase in series and a PMMA2 phase in parallel. The PDMS phase is arranged in series with the PMMA1 phase and parallel to the PMMA2 phase. The total normalized permeation rate (P) in the combined model is given by eq 1:

$$P = (\phi_{\mathrm{PDMS}} + \phi_{\mathrm{PMMA1}})^2 \times \frac{P_{\mathrm{PMMA}}P_{\mathrm{PDMS}}}{\phi_{\mathrm{PDMS}}P_{\mathrm{PMMA}} + \phi_{\mathrm{PMMA1}}P_{\mathrm{PDMS}}} + \phi_{\mathrm{PMMA2}}P_{\mathrm{PMMA}} \quad (1)$$

$$\phi_{\mathrm{PMMA1}} + \phi_{\mathrm{PMMA2}} + \phi_{\mathrm{PDMS}} = 1$$

The purpose of this section is to quantitatively follow the morphological changes in microphase separation of the original and annealed PMMA-*b*-PDMS membranes. Therefore, the volume fractions of the PMMA1 and PMMA2 phases (ϕ_{PMMA1}, ϕ_{PMMA2}) were determined from the experimental normalized permeation rates (P_{PMMA}, P_{PDMS}) of an aqueous ethanol solution using eq 1, after the volume fraction of the PDMS phase, ϕ_{PDMS}, was calculated on the basis of the known DMS content in the copolymer. The results for the original and annealed PMMA-*b*-PDMS membranes as a function of the annealing temperature are shown in Figure 5. In the PMMA-*b*-PDMS membranes with a DMS content of 29 and 62 mol %, the volume fractions of the PMMA1 and PMMA2 phases were kept constant with rising temperature. In the membranes with a DMS content of 41 mol %, however, the volume fraction of the PMMA1 phase decreased and the volume fraction of the PMMA2 phase increased gradually. Because the PMMA1 phase is arranged in series with the PDMS phase and the PMMA2 phase is in parallel to the PDMS phase, the changes in the PMMA volume fractions of the membrane with a DMS content of 41 mol % mean that the structural model for the permeation of an aqueous ethanol solution changes from a series model to a parallel model. In addition, the volume fraction of the PMMA1 phase in the membrane with a DMS content of 62 mol % PDMS was almost zero. This result suggests

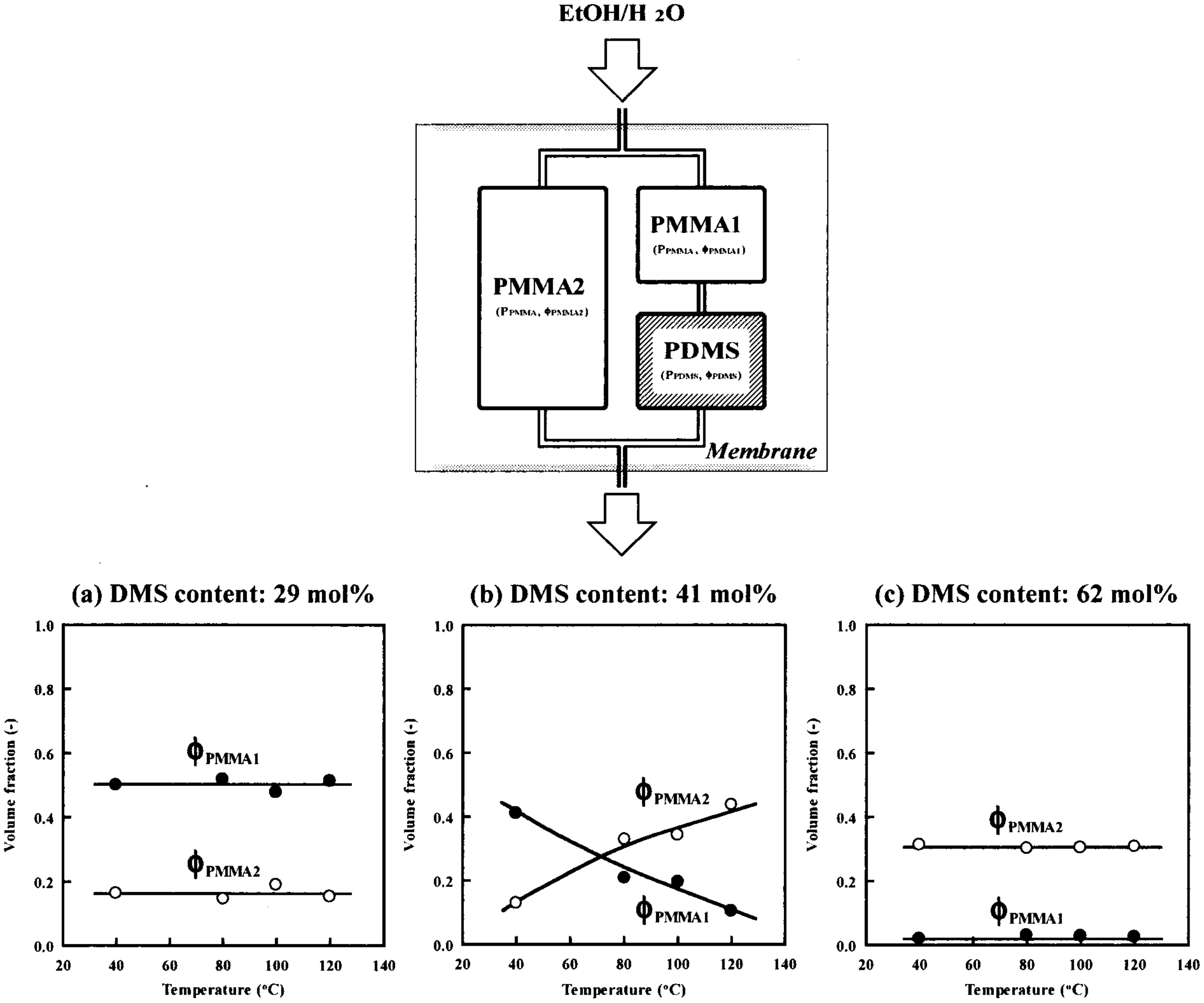

(a) DMS content: 29 mol%

(b) DMS content: 41 mol%

(c) DMS content: 62 mol%

Figure 5. Relationship between the annealing temperature and the volume fraction of the elements in a combined model consisting of both a series model and a parallel model for the annealed PMMA-*b*-PDMS membranes with DMS contents of 29 (a), 41 (b), and 62 mol % (c): ●, volume fraction of the PMMA element in the series model (ϕ_{PMMA1}); ○, volume fraction of the PMMA element in the parallel model (ϕ_{PMMA2}).

that it had microphase separation characteristics corresponding to a parallel model. Consequently, it is easily concluded that rising annealing temperature resulted in a morphological change from a discontinuous PDMS phase to a continuous PDMS phase in the direction of the membrane thickness.

Figure 6 shows the effect of the DMS content on the volume fractions of elements in a combined model for the original PMMA-*b*-PDMS membranes and their membranes annealed at 120 °C for 2 h. More remarkable is the change in the volume fraction of the PMMA1 phase, which is arranged in series with the PDMS phase. In both the original and annealed membranes, the volume fraction of the PMMA1 phase showed a sharp decrease with increasing DMS content. The volume fraction of the PMMA1 phase in the original PMMA-*b*-PDMS membranes approached zero at a DMS content above 60 mol %, but the volume fraction in the annealed PMMA-*b*-PDMS became zero at over 40 mol %. Furthermore, the volume fraction of the PMMA2 phase, which is arranged in parallel with the PDMS phase, increased abruptly in both the original and annealed PMMA-*b*-PDMS membranes at a DMS content of about 55 and 37 mol %, respectively. The changes in the PMMA1 and PMMA2 phases suggest that the overall structural model for the permeation through the original and annealed PMMA-*b*-PDMS membranes changes from a series model to a parallel model at a DMS content of 55 and 37 mol %, respectively. Therefore, the original and annealed PMMA-*b*-PDMS membranes at a DMS content of less than 55 and 37 mol %, respectively, have microphase separation characteristics corresponding to a series model, but the original membranes with over 55 mol % DMS and annealed membranes with over 37 mol % DMS have microphase separation corresponding to a parallel model.

On the basis of the discussion of the microphase separation using the combined model, it is easily understood that the PDMS phase changes from a discontinuous phase to a continuous phase in the direction of the membrane thickness at the corresponding DMS content. This suggestion is consistent with the aforementioned conclusion from TEM observations. At a DMS content between 37 and 55 mol %, the annealing gives rise to a considerable change in the morphology of the microphase separation in the PMMA-*b*-PDMS membranes. In other words, these results suggest that the PDMS component forms a continuous phase more readily during the annealing because of enhanced mobility of the polymer chains. It is worth noting that both the original and annealed membranes changed from water- to ethanol-permselective at the DMS content corresponding to a structural change from a series model to a parallel model.

(a) PMMA-*b*-PDMS membrane

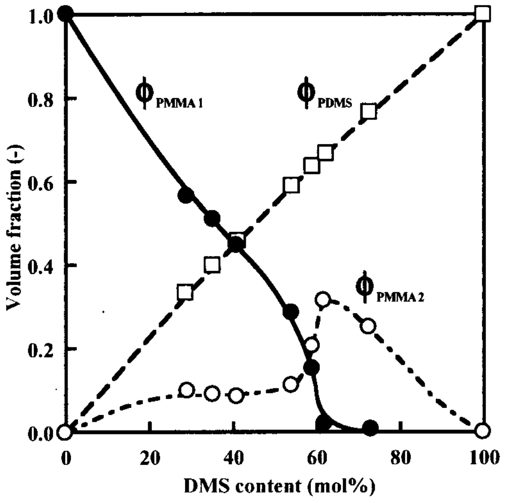

(b) Annealed PMMA-*b*-PDMS membrane

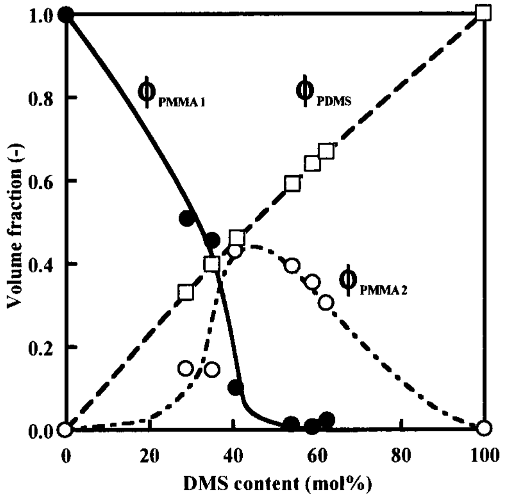

Figure 6. Relationship between the DMS content and the volume fraction of the elements in a combined model consisting of both a series model and a parallel model for the PMMA-*b*-PDMS membranes (a) and their annealed membranes (120 °C, 2 h) (b): ●, volume fraction of the PMMA element in the series model (ϕ_{PMMA1}); ○, volume fraction of the PMMA element in the parallel model (ϕ_{PMMA2}); □, volume fraction of the PDMS element in the parallel model (ϕ_{PDMS}).

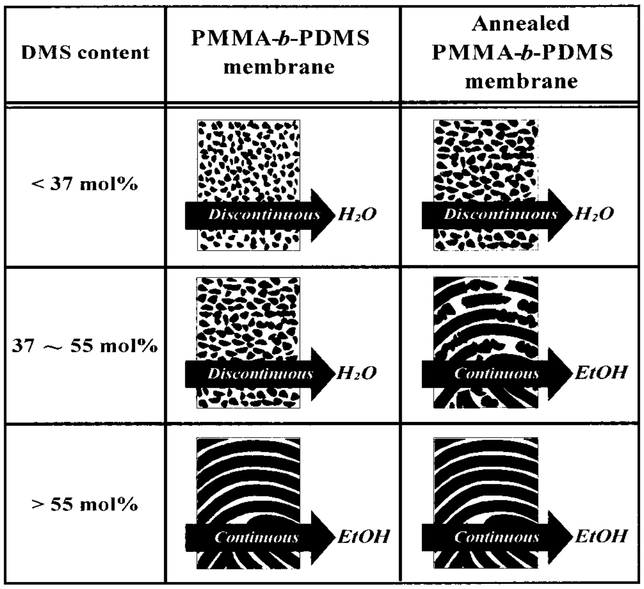

Figure 7. Tentative illustration of the relationship between the microphase separation in the original and annealed PMMA-*b*-PDMS membranes and their permselectivity for an aqueous ethanol solution.

Consequently, these morphological changes can be directly related to the permselectivity for an aqueous ethanol solution through the original and annealed PMMA-*b*-PDMS membranes during pervaporation as follows (Figure 7). A PMMA homopolymer membrane is water-permselective because of higher diffusivity of water molecules than ethanol molecules, and a PDMS homopolymer membrane is ethanol-permselective because of the relatively stronger affinity of PDMS for ethanol than water. Because the permselectivity of microphase-separated membranes having a discontinuous PDMS phase is governed by the water-permselectivity of the continuous PMMA phase, the membranes are water-permselective. However, after the PDMS component forms a continuous phase in the direction of the membrane thickness with increasing DMS content, the ethanol-permselectivity of the PDMS phase subsequently becomes more predominant than the water-permselectivity of the PMMA phase. This is due to the fact that the permeants are preferentially diffusing in the PDMS phase because of the low T_g of this phase. Thus, the original PMMA-*b*-PDMS membranes change from water-permselectivity to ethanol-permselectivity at a DMS content of 55 mol %, at which a PDMS phase in their microphase separation changes strongly from a discontinuous phase to a continuous phase. On the other hand, the annealing at 120 °C results in dramatic changes in morphology of the PMMA-*b*-PDMS membranes with a DMS content between 37 and 55 mol %. It is apparent from the TEM observation and the analysis with a combined model that the PDMS component in the annealed PMMA-*b*-PDMS membrane forms a continuous phase at a DMS content of more than 37 mol %. The formation of the continuous PDMS phase by the annealing causes a shift in the threshold DMS content at which the ethanol-permselectivity of the PMMA-*b*-PDMS membrane is strongly enhanced. These conclusions suggest that the annealing enables us to control the morphology of microphase separation in multicomponent polymer membranes and to improve their pervaporation characteristics. In the next section, furthermore, we focus on differences in the annealing effect on the permeability and permselectivity between the block and graft copolymer membranes.

Comparison of Annealing Effect between PMMA-*b*-PDMS and PMMA-*g*-PDMS Membranes. A previous paper revealed that a difference in morphology between the block and graft copolymer membranes, which is strongly governed by the molecular architecture, causes their quite different permeability and permselectivity for an aqueous ethanol solution.[19] In this section, the effect of the annealing on the microphase separation and pervaporation characteristics of the graft copolymer membranes (PMMA-*g*-PDMS) is compared with the annealing effect for the block copolymer membranes (PMMA-*b*-PDMS). Figure 8 shows the relationship between the DMS content and the pervaporation characteristics for an aqueous solution of 10 wt % ethanol through the original PMMA-*g*-PDMS membranes and their membranes annealed at 120 °C for 2 h. Similarly to the pervaporation characteristics of the PMMA-*b*-PDMS membranes shown in Figure 2,

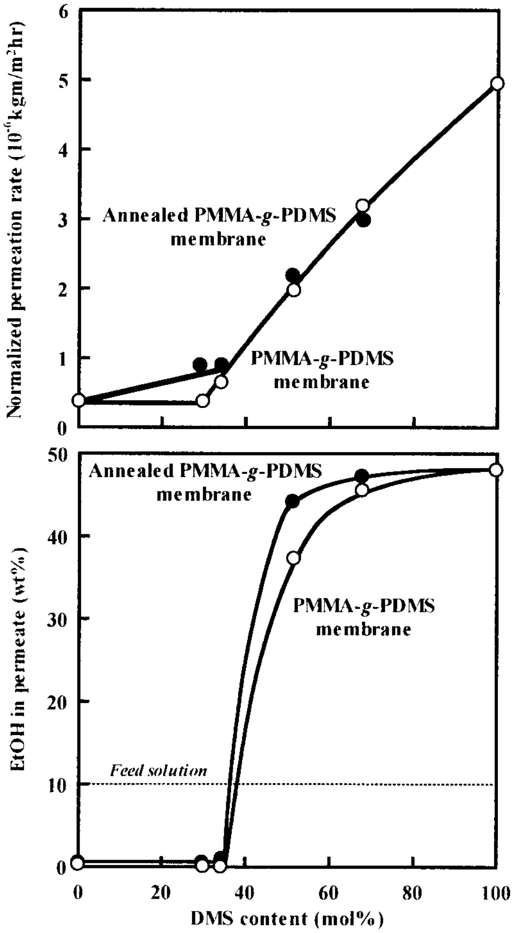

Figure 8. Effects of the DMS content on the ethanol concentration of the permeate and on the normalized permeation rate through the PMMA-*g*-PDMS membranes (○) and their annealed membranes (120 °C, 2 h) (●) during pervaporation. The feed solution was an aqueous solution of 10 wt % ethanol (40 °C). The dashed line represents the feed composition.

the ethanol concentration in the permeate and the normalized permeation rate increased with increasing DMS content. As reported in a previous paper,[19] the threshold DMS content at which the permeability and permselectivity of the original PMMA-*g*-PDMS membranes changed abruptly was much lower than the threshold DMS content for the original PMMA-*b*-PDMS membranes. Although the annealing enhanced the ethanol-permselectivity of the PMMA-*g*-PDMS membranes slightly, the threshold DMS content at which the pervaporation characteristics of the PMMA-*g*-PDMS membranes changed strongly did not change at all due to the annealing. Thus, the annealing of the PMMA-*b*-PDMS membranes shifted the threshold DMS content for the pervaporation characteristics, but the annealing of the PMMA-*g*-PDMS did not. It is apparent that the threshold DMS contents for the original and annealed PMMA-*b*-PDMS membranes were 55 and 37 mol %, respectively, and the threshold of both the original and annealed PMMA-*g*-PDMS was 37 mol %.

To clarify the reason why the annealing of the PMMA-*g*-PDMS membranes did not shift the threshold DMS content for their pervaporation characteristics, the annealing effect on their membrane structures was investigated in the same way as in the case of the PMMA-*b*-PDMS membranes. Figure 9 shows the effect of the DMS content on the contact angles of water on the original PMMA-*g*-PDMS membranes and their membranes annealed at 120 °C for 2 h. Predictably, the contact angles on the air-side surface were much larger than those on the glass-side surface. This is due to the fact that the more hydrophobic PDMS component was readily localized to the air-side surface and the less hydrophobic PMMA component was concentrated to the glass-side surface for the minimization of the surface and interfacial free energy. Differing from the surface characteristics of the PMMA-*b*-PDMS membranes, there was no difference in the contact angles of water on the air- and glass-side surfaces between the original and annealed PMMA-*g*-PDMS membranes. This means that the annealing did not lead to a change in the surface structures of the PMMA-*g*-PDMS membranes. Thus, the effect of the annealing on the surface structures of the PMMA-*g*-PDMS membranes is quite different from that of the PMMA-*b*-PDMS membranes.

(a) Air-side surface

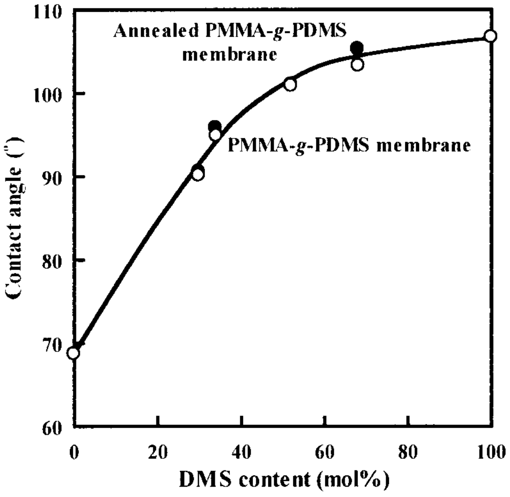

(b) Glass-side surface

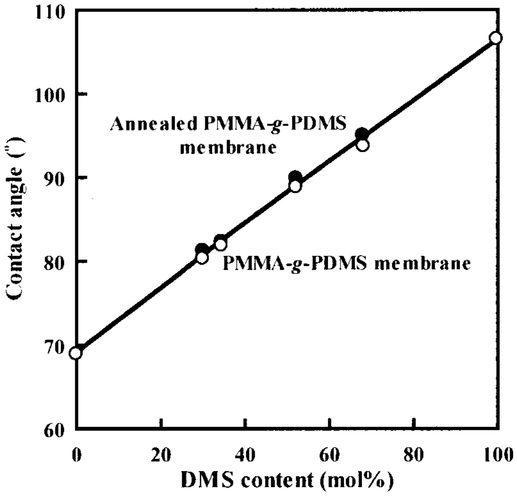

Figure 9. Effects of the DMS content on the contact angle of water on the air-side surface (a) and glass-side surface (b) of PMMA-*g*-PDMS membranes (○) and their annealed membranes (120 °C, 2 h) (●).

Figure 10 shows the TEM images of the PMMA-*g*-PDMS membranes and their membranes annealed at 120 °C for 2 h. These images demonstrate that both the original and annealed PMMA-*g*-PDMS membranes had microphase-separated structures which were quite different from those of the original and annealed PMMA-*b*-PDMS membranes. In addition, it was observed that

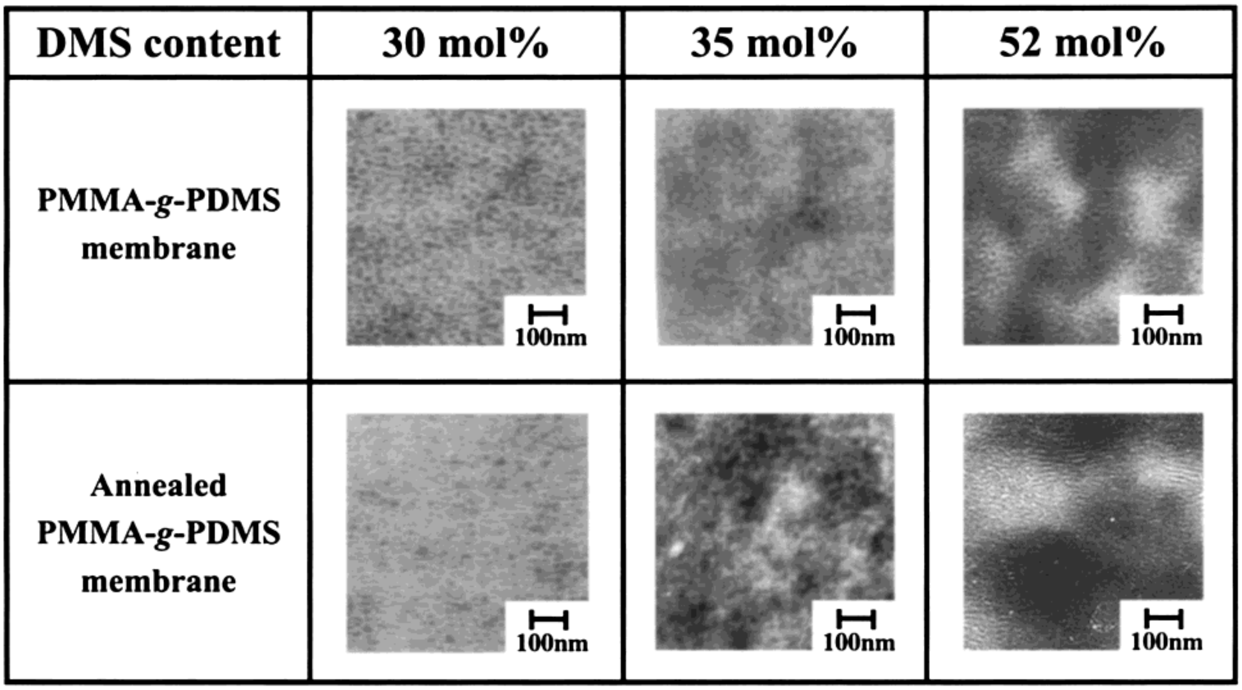

Figure 10. Transmission electron micrographs of cross sections of the PMMA-*g*-PDMS membranes and their annealed membranes (120 °C, 2 h) with various DMS contents. The dark region stained by RuO_4 represents the PDMS component.

the morphology of the microphase separation in the original PMMA-*g*-PDMS membranes was very similar to that in their annealed membranes. As a result, it can be concluded that the annealing of the PMMA-*b*-PDMS membranes results in dramatic changes in the morphology of their microphase separation but that of the PMMA-*g*-PDMS membrane does not.

As shown in Figure 11, furthermore, the analysis using the combined model shown in Figure 5 demonstrated very little effect of the annealing on the microphase separation of the PMMA-*g*-PDMS membranes. In both the original and annealed PMMA-*g*-PDMS membranes, the volume fraction of the PMMA1 phase approaches zero, and the volume fraction of the PMMA2 phase increased abruptly at a DMS content of about 37 mol %. This means that the structural model for both the original and annealed PMMA-*g*-PDMS membranes changes from a series model to a parallel model at a DMS content of about 37 mol %, regardless of the annealing. In other words, both the original and annealed graft copolymer membranes with a DMS content of more than 37 mol % have a microphase separation consisting of a continuous PDMS phase, similarly to the annealed PMMA-*b*-PDMS membranes with a DMS content of more than 37 mol %. Consequently, the morphology of the microphase separation in the PMMA-*g*-PDMS membranes is little influenced by the annealing, differing from the morphology of the PMMA-*b*-PDMS membranes in which the annealing shifts the threshold DMS content. This is attributable to the fact that the difference in the molecular architecture between the block and graft copolymers induces different morphology of the microphase separation which has specifically stable states. In the PMMA-*b*-PDMS membranes, the shift of the threshold DMS content to 37 mol % by the annealing means that the morphology of a continuous PDMS phase is thermodynamically most stable in the PMMA-*b*-PDMS membranes with a PDMS content of more than 37 mol %. Furthermore, no morphological change in the PMMA-*g*-PDMS membranes due to the annealing implies that the original PMMA-*g*-PDMS membranes have a very stable morphology in which the PDMS phase is continuous at a DMS content over 37 mol %. These results lead us to the conclusion that the morphology having a continuous PDMS phase is the most stable in two-component polymer membranes with a DMS content of more than 37 mol %, regardless of the molecular architecture like block and graft copolymers. However, because not all of the membranes form the most stable morphology during membrane formation, the annealing results in dramatic morphological changes in some membranes due to the high mobility of the polymer chains.

The molecular architecture determines how readily the most stable morphology is formed during the membrane formation. The PDMS segments in the graft copolymer membranes are probably assembled more quickly and easily than those of the block copolymer membranes because the former has a free PDMS segment end and the latter has both the PDMS segment ends fixed in the backbone chains. This must lead to a more stable microphase separation in the graft copolymer membranes than in the block copolymer membranes. Therefore, the annealing of the graft copolymers having stable morphology results in no morphological change in their microphase separation. In some block copolymer membranes, however, the stable morphology is not formed during membrane formation due to the lower mobility of the PDMS segment in the block copolymer than in the graft copolymer. In addition, both the PDMS segment ends fixed in the block copolymer backbone may cause their well-defined morphology, i.e., bicontinuous phases. Thus, the annealing of the block copolymer membranes leads to more stable morphology having bicontinuous phases as shown in Figure 4.

As reported in previous papers,[12−19] the morphology of the microphase separation in multicomponent polymer membranes influences their permeability and permselectivity strongly. Therefore, when the PDMS component begins to form a continuous phase on an-

(a) PMMA-*g*-PDMS membrane

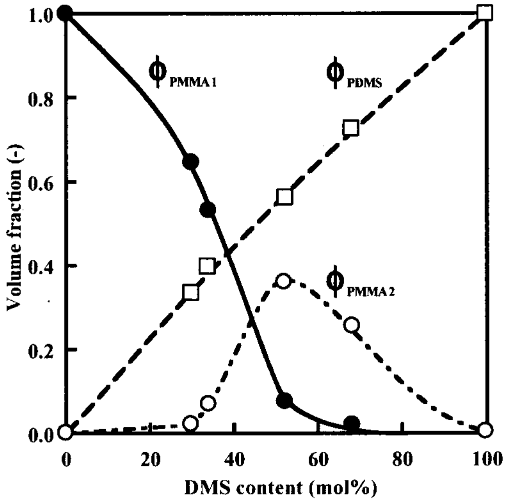

(b) Annealed PMMA-*g*-PDMS membrane

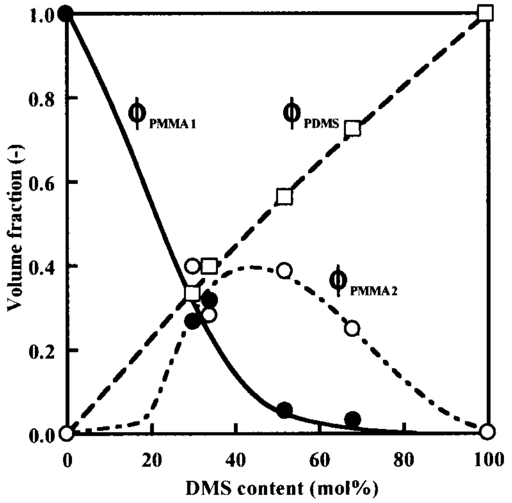

Figure 11. Relationship between the DMS content and the volume fraction of the elements in a combined model consisting of both a series model and a parallel model for the PMMA-*g*-PDMS membranes (a) and their annealed membranes (120 °C, 2 h) (b): ●, volume fraction of the PMMA element in the series model (ϕ_{PMMA1}); ○, volume fraction of the PMMA element in the parallel model (ϕ_{PMMA2}); □, volume fraction of the PDMS element in the parallel model (ϕ_{PDMS}).

nealing, the microphase-separated membranes change from water-permselectivity to ethanol-permselectivity because their permselectivity is strongly governed by the continuous PDMS phase that is ethanol-permselective. As a result, the annealing of the PMMA-*b*-PDMS membranes changes their permeability and permselectivity for an aqueous ethanol solution in pervaporation due to their morphological change, but the annealing of the PMMA-*g*-PDMS membrane does not. This study leads us to the conclusion that designing microphase separation in multicomponent polymer membranes by controlling molecular architecture and annealing is of great importance for the development of high-performance pervaporation membranes.

Conclusions

The annealing of the PMMA-*b*-PDMS membranes having microphase-separated structures enhanced their permeability and permselectivity in the separation of an aqueous ethanol solution by pervaporation. The original PMMA-*b*-PDMS membranes changed abruptly from water- to ethanol-permselectivity at a DMS content of 55 mol %. However, the threshold DMS content, at which the membrane permselectivity changed dramatically, was shifted from 55 to 37 mol % following the annealing of the PMMA-*b*-PDMS membranes. It was apparent from TEM observations that the annealing gives rise to a morphological change in the microphase separation of the PMMA-*b*-PDMS membranes with a PDMS content between 37 and 55 mol %. At a PDMS content between 37 and 55 mol %, the original and annealed PMMA-*b*-PDMS membranes had a microphase separation with discontinuous and continuous PDMS phases, respectively. The morphological changes in the PMMA-*b*-PDMS membranes due to the annealing were also discussed by the analysis using a combined model consisting of series and parallel models. Consequently, the formation of a continuous PDMS phase by the annealing of the PMMA-*b*-PDMS membranes causes the enhancement of their ethanol-permselectivity. Furthermore, the annealing effect on the pervaporation characteristics of the PMMA-*g*-PDMS membranes was compared with the annealing effect of the PMMA-*b*-PDMS membranes. There was very little effect of the annealing on the permeability and permselectivity of the PMMA-*g*-PDMS membranes, differing from the PMMA-*b*-PDMS membranes. This is due to no morphological change in the microphase separation of the PMMA-*g*-PDMS membranes as a result of the annealing. These results led us to conclude that the permeability and permselectivity of multicomponent polymer membranes are strongly governed by the morphology of their microphase separation, which can be controlled by their molecular architecture and their annealing. The threshold DMS content at which pervaporation characteristics change dramatically was closely associated with the DMS content at which the PDMS component changed from a discontinuous phase to a continuous phase, regardless of the molecular architecture. The results of this study revealed the detailed relationship between the microphase separation and the permselectivity of multicomponent polymer membranes and provided a basis for designing the structure of high-performance pervaporation membranes.

References and Notes

(1) Huang, R. Y. M. *Pervaporation Membrane Separation Processes*; Elsevier: Amsterdam, 1991.
(2) Takegami, S.; Yamada, H.; Tsujii, S. *J. Membr. Sci.* **1992**, *75*, 93.
(3) Okamoto, K.; Butsuen, A.; Tsuru, S.; Nishioka, S.; Tanaka, K.; Kita, H.; Asaoka, S. *Polym. J.* **1987**, *19*, 747.
(4) Ishihara, K.; Nagase, Y.; Matsui, K. *Makromol. Chem., Rapid Commun.* **1986**, *7*, 43.
(5) Nagase, Y.; Mori, S.; Matsui, K. *J. Appl. Polym. Sci.* **1989**, *37*, 1259.
(6) Nagase, Y.; Ishihara, K.; Matsui, K. *J. Polym. Sci., Polym. Phys. Ed.* **1990**, *28*, 377.
(7) Nagase, Y.; Sugimoto, K.; Takamura, Y.; Matsui, K. *J. Appl. Polym. Sci.* **1991**, *43*, 1227.
(8) Uragami, T.; Matsuda, T.; Nishimoto, H.; Miyata, T. *J. Membr. Sci.* **1994**, *88*, 243.
(9) Uragami, T.; Kato, S.; Miyata, T. *J. Membr. Sci.* **1997**, *124*, 203.
(10) Inui, K.; Tsukamoto, K.; Miyata, T.; Uragami, T. *J. Membr. Sci.* **1998**, *138*, 67.
(11) Uragami, T.; Tsukamoto, K.; Inui, K.; Miyata, T. *Macromol. Chem. Phys.* **1998**, *199*, 49.
(12) Miyata, T.; Takagi, T.; Kadota, T.; Uragami, T. *Macromol. Chem. Phys.* **1995**, *196*, 1211.
(13) Miyata, T.; Higuchi, J.; Okuno, H.; Uragami, T. *J. Appl. Polym. Sci.* **1996**, *61*, 1315.

(14) Miyata, T.; Takagi, T.; Uragami, T. *Macromolecules* **1996**, *29*, 7787.

(15) Miyata, T.; Nakanishi, Y.; Uragami, T. *Macromolecules* **1997**, *30*, 5563.

(16) Miyata, T.; Nakanishi, Y.; Uragami, T. *ACS Symp. Ser.*, in press.

(17) Uragami, T.; Doi, T.; Miyata, T. *ACS Symp. Ser.*, in press.

(18) Miyata, T.; Takagi, T.; Higuchi, J.; Uragami, T. *J. Polym. Sci., Polym. Phys.* **1999**, *37*, 1545.

(19) Miyata, T.; Obata, S.; Uragami, T. *Macromolecules* **1999**, *32*, 3712.

(20) Miyata, T.; Iwamoto, T.; Uragami, T. *J. Appl. Polym. Sci.* **1994**, *51*, 2007.

(21) Miyata, T.; Iwamoto, T.; Uragami, T. *Macromol. Chem. Phys.* **1996**, *197*, 2909.

(22) Inui, K.; Miyata, T.; Uragami, T. *J. Polym. Sci., Polym. Phys.* **1997**, *35*, 699.

(23) Inui, K.; Okazaki, K.; Miyata, T.; Uragami, T. *J. Membr. Sci.* **1998**, *143*, 93.

(24) Inui, K.; Miyata, T.; Uragami, T. *J. Polym. Sci., Polym. Phys.* **1998**, *36*, 281.

(25) Inui, K.; Miyata, T.; Uragami, T. *Macromol. Chem. Phys.* **1998**, *199*, 589.

(26) Kempner, D.; Frisch, K. C. *Polymer Alloys III*; Plenum: New York, 1981.

(27) Aggarwal, S. L. In *Processing, Structure and Properties of Block Copolymers*; Folkes, M. J., Ed.; Elsevier: New York, 1985; p 1.

(28) Paul, D. R. In *Multicomponent Polymer Materials*; Paul, D. R., Sperling, L. H., Eds.; American Chemical Society: Washington, DC, 1986; p 3.

(29) Prentice, P.; Papapostolou, E.; Williams, J. G. In *Multicomponent Polymer Material*; Paul, D. R., Sperling, L. H., Eds.; American Chemical Society: Washington, DC, 1986; p 325.

(30) Sperling, L. H. *Polymeric Multicomponent Materials: an Introduction*; John Wiley & Sons: New York, 1997.

(31) Crank, J.; Park, G. S. *Diffusion in Polymers*; Academic Press: New York, 1968.

(32) Barrie, J. A.; Munday, K. *J. Membr. Sci.* **1983**, *13*, 175.

(33) Barrie, J. A.; William, M. J. L.; Spencer, H. *J. Membr. Sci.* **1984**, *21*, 185.

(34) Barrie, J. A.; Sagoo, P.; Thomas, A. G. *J. Membr. Sci.* **1989**, *43*, 229.

(35) Robeson, L. M.; Noshay, A.; Matzner, M.; Merriam, C. M. *Angew. Makromol. Chem.* **1973**, *29/30*, 47.

(36) Barnabeo, A. E.; Creasy, W. S.; Robeson, L. M. *J. Polym. Sci., Polym. Chem. Ed.* **1975**, *13*, 1979.

(37) Tsujita, Y.; Yoshimura, K.; Yoshimizu, H.; Takizawa, A.; Kinoshita, T. *Polymer* **1993**, *34*, 2597.

(38) Fujimoto, T.; Ohkoshi, K.; Miyaki, Y.; Nagasawa, M. *J. Membr. Sci.* **1984**, *20*, 313.

(39) Lerma, M. S.; Iwamoto, K.; Seno, M. *J. Appl. Polym. Sci.* **1987**, *33*, 625.

(40) Chiou, J. S.; Paul, D. R. *J. Appl. Polym. Sci.* **1987**, *33*, 2935.

(41) Lee, Y. K.; Tak, T.-M.; Lee, D. S.; Kim, S. C. *J. Membr. Sci.* **1990**, *52*, 157.

(42) Lee, D. S.; Jung, D. S.; Kim, T. H.; Kim, S. C. *J. Membr. Sci.* **1991**, *60*, 233.

(43) Lee, D. S.; Kang, W. K.; An, J. H.; Kim, S. C. *J. Membr. Sci.* **1992**, *75*, 15.

(44) Kerres, J. A.; Strathmann, H. *J. Appl. Polym. Sci.* **1993**, *50*, 1405.

(45) Inoue, H.; Ueda, A.; Nagai, S. *J. Polym. Sci., Part A: Polym. Chem.* **1988**, *26*, 1077.

(46) Inoue, H.; Ueda, A.; Nagai, S. *J. Appl. Polym. Sci.* **1988**, *35*, 2039.

(47) Inoue, H.; Matsumoto, A.; Matsukawa, K.; Ueda, A. *J. Appl. Polym. Sci.* **1990**, *40*, 1917.

(48) Trent, J. S.; Scheinbeim, J. I.; Couchman, P. R. *Macromolecules* **1983**, *16*, 589.

(49) Moe, M. B.; Koros, W. J.; Paul, D. R. *J. Polym. Sci., Polym. Phys.* **1988**, *26*, 1931.

(50) Coll, H.; Searles, C. G. *Polymer* **1988**, *29*, 1266.

(51) Noll, W. In *Chemistry and Technology of Silicones*; Academic Press: New York, 1968.

(52) Kesting, R. E.; Fritzsche, A. K. *Polymeric Gas Separation Membranes*; John Wiley & Sons: New York, 1993.

(53) Plate, N.; Yampol'skii, Y. P. In *Polymeric Gas Separation Membranes*; Paul, D. R., Yampol'skii, Y. P., Eds.; CRC Press: London, 1994; p 155.

MA9909612